ACADEMIA ROMÂNĂ
Revue Roumaine de Chimie
http://web.icf.ro/rrch/

Rev. Roum. Chim.,
2014, *59*(10), 867-874

GLUTATHIONE-BASED SILVER NANOPARTICLES WITH DUAL BIOMEDICAL ACTIVITY

Manuela MURARIU,[a,b] Iuliana STOICA,[a] Robert GRADINARU,[b]
Gabi DROCHIOIU,[b,*] and Ionel MANGALAGIU[b,*]

[a] Petru Poni Institute of Macromolecular Chemistry, 41a Grigore Ghica Voda Alley, Iaşi-700487, Roumania
[b] Faculty of Chemistry, Al. I. Cuza University of Iaşi, 11 Carol I, Iaşi-700506, Roumania

Received September 5, 2014

We report herein a feasible study concerning synthesis, characterization and potential biomedical applications of silver nanoparticles with glutathione skeleton. The synthesis of nanoparticles is facile and efficient, using silver nitrate as the starting material, sodium borohydride as reducing agent and glutathione. The characterization of glutathione-stabilized Ag-NPs (GS-Ag-NPs) as well as the Ag-NPs used for comparison was performed by FT-IR, UV-VIS, AFM and SEM techniques. Ag-NPs were biologically active at concentrations less than 10^{-4} M, whereas GS-Ag-NPs were ineffective at the same concentrations. Moreover, depending on the particles size, 10^{-6} M concentrations of Ag-NPs stimulated microorganism growth, whereas the more concentrated suspensions (10^{-4} M) inhibited *Escherichia coli* (*E. coli*) growth. The biological implications of our data are discussed in the frame of current literature.

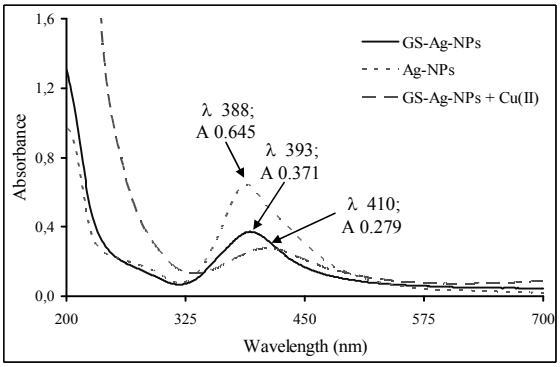

INTRODUCTION

The metal nanoparticles are used in bioapplications as therapeutics, transfection vectors, and fluorescent labels.[1-4] Properties of metal nanoparticles are different from those of bulk materials made of the same atoms.[5] Stable nanosize silver particles were spontaneously formed by reduction of aqueous metal salt solutions in the presence of sugar-persubstituted poly(amidoamine) dendrimers.[6] However, most authors report on the reaction of silver nitrate with sodium citrate.[7] Besides, a simple, green method was developed for the synthesis of gold and silver nanoparticles by using polysaccharides as reducing/stabilizing agents.[8] Noble metal nanoparticles can also be obtained by evaporation of atoms on a metal surface using high energy laser, followed by cooling them with nanoparticle formation[9,10] or microwaves in the presence of poly (N-vinyl-2-pyrrolidone).[11] In principle, the chemical agents commonly used to reduce silver ions are: aldehydes,[12] sugars,[8] hydrazine, H_3PO_2, $NaBH_4$ and sodium citrate. Thus, silver nanoparticles can be synthesized by several methods such as chemical reduction using a reducing agent,[13-20] or photochemical reduction.[21,22] A biological synthesis of quasi-spherical silver nanoparticles by using active pharmaceutical ingredients as the reducing and stabilizing agent was also reported.[23] Controlling the size, shape, and structure of silver nanoparticles is technologically important because of the strong correlation between these parameters and optical, electrical, and their catalytic properties.[24]

* Corresponding authors: gabidr@uaic.ro and ionelm@uaic.ro

In addition to their medical uses, Ag-NPs are also used in clothing, the food industry, paints, electronics and other fields.[25-28] Despite their widespread use, there is a serious lack of information concerning the toxicity of Ag-NPs to humans and their underlying cellular actions. Nevertheless, some studies have shown that Ag-NPs accumulation in the liver could induce cytotoxicity via oxidative cell damage.[29-31] However, silver nanoparticles exhibit cytoprotection towards HIV-1 infected cells,[32,33] and also have the ability to modulate the cytokines involved in wound healing. A specific and protective role for silver ions in brain pathologies was related to their high affinity toward physiologically and pharmacologically active peptides, and their conformation change to large α-helices during silver binding.[34]

Glutathione (GSH) is a tripeptide (γ-Glu-Cys-Gly) which contains a –SH group. This peptide can be easily adsorbed onto the surface of metal nanoparticles. GSH can bind heavy metals, solvents, and pesticides to be excreted in urine or bile.[35] Several studies have recently been performed to understand the reactivity of glutathione in the presence of nanoparticles.[36] Glutathione proved to diminish the radiotoxic effect of radioactive mercury, whereas cystine had also a powerful protective effect.[37-38]

In spite of all these investigations, it is not yet clear how bacteria can interact with noble metal nanoparticles, and the relationship which is between the nanomaterial production and its antibacterial activity as well as the effect of glutathione and the reducing agents on the biological activity of the resulted nanomaterials.

Our study reports on the synthesis and the effect of silver nanoparticles on cellular growth of *Escherichia coli* (*E. coli*). In addition, we outline the impact of glutathione functionalization of these nanoparticles on living microorganisms in view of further biological applications.

RESULTS AND DISCUSSION

Characterization of nanoparticles. The newly synthesized silver nanoparticles were characterized by SEM and AFM techniques, as well as FT-IR and UV-visible spectroscopy. The size of the obtained nanoparticles was found to be dependent on the procedure used to produce nanoparticles. On increasing temperature and decreasing the reaction time, smaller nanoparticles were obtained, whereas their absorption maximum shifts to shorter wavelengths. In addition, the nanoparticles partly aggregated to form larger aggregates (over 100 nm), which were removed by centrifugation. Most Ag-NPs were 5-10 nm in size as SEM image revealed (Fig. 1).

However, we produced 10-14 nm-sized nanoparticles from silver having an absorption maximum of 388 nm (Fig. 2). Glutathione binding to Ag-NPs induced a decrease in the absorption maximum from 0.645 to 0.393; the maximum was shifted to longer wavelengths by 5 nm. Copper ion reaction with the glutathione bound on the particle surface produced an additional shift to 410 nm, indicating an increase in the particle size.

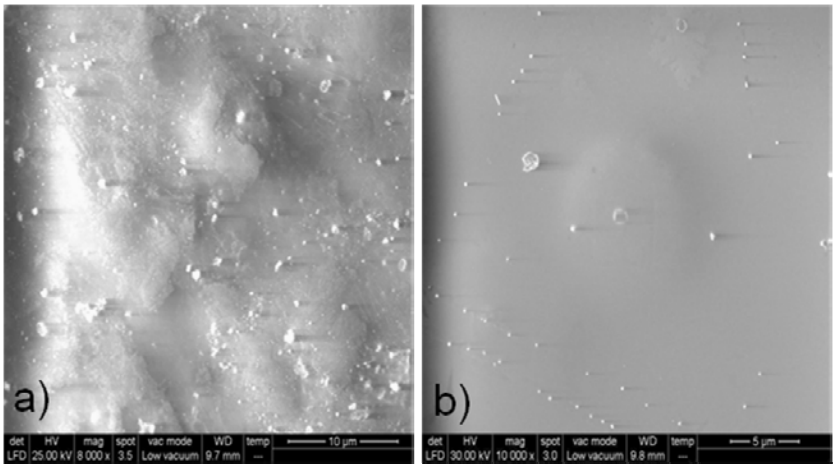

Fig. 1 – SEM images of a) silver nanoparticles (Ag-NPs) and b) glutathione-stabilized silver nanoparticles (GS-Ag-NPs).

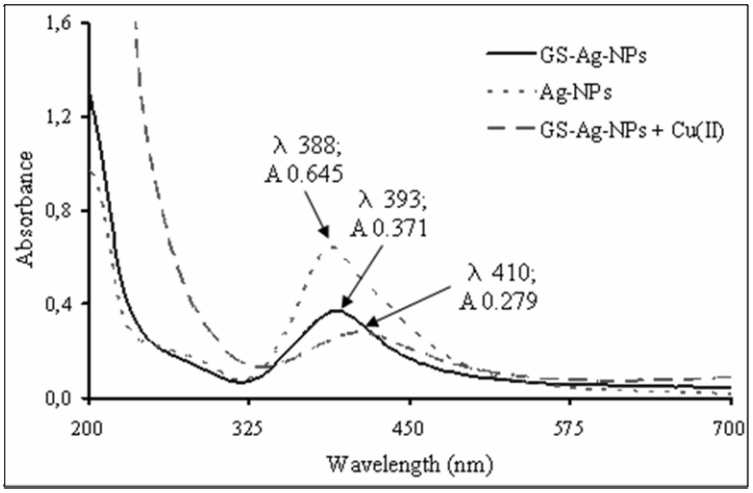

Fig. 2 – UV-Vis absorption spectra of silver nanoparticles as well as the glutathione-stabilized ones (C = 250 μM).

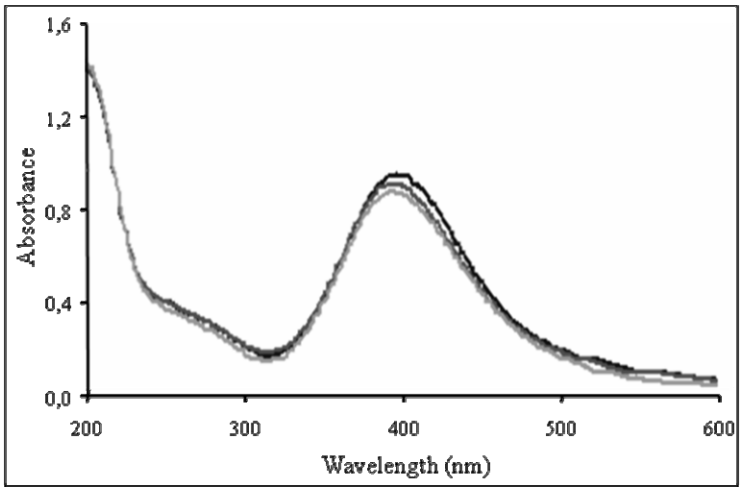

Fig. 3 – Stability of GS-Ag-NPs: blue – immediately after synthesis, red – 48 hours later, green – 96 hours later.

We found only the reduced form of glutathione (4% of initial GSH, the rest was probably bound to Ag-NPs). No oxidized glutathione was found. Therefore, the microorganisms used in the biological experiments are expected to interact with nanoparticle surface or with the glutathione bound to the nanoparticles. Once obtained, the resulted nanoparticles were centrifuged for 10 min at 6000 rpm, yet no pellet was observed. The obtained nanoparticles were also stable for a long time in solution, at room temperature. The suspensions of newly synthesized GS-Ag-NPs were stable up to several weeks (Fig. 3).

Within another experiment, we noticed that glutathione does not change the absorbance of the colloidal solution of gold nanoparticles. However, the intense absorption at 210-220 nm revealed the presence of unbound glutathione. On the contrary, silver nanoparticles showed a characteristic absorption maximum at 388 nm and an additional absorption band at 524 nm, specific to larger nanoparticles (Fig. 4). Besides, this band was also observed but at lower concentrations (0.25 mM) and not at 1 mM, suggesting a process of nanoparticle aggregation. Following glutathione binding, the absorption band at 524 nm disappeared.

FT-IR Spectroscopy. On comparing the spectrum of pure GSH with that of GS-Ag-NPs, a significant change was observed. The characteristic signal at 2524 cm^{-1} of SH group in the molecule of glutathione disappeared, denoting the formation of a S-Ag bond (Fig. 5) or a S-S one. Since oxidized glutathione was not detected in the presence of the GS-Ag-NPs, GSH was probably modified onto the surface of silver nanoparticles via the reaction of thiol group in the cysteine moiety of GSH with silver ion. Our results are in agreement with those previously reported in the literature.[40, 41]

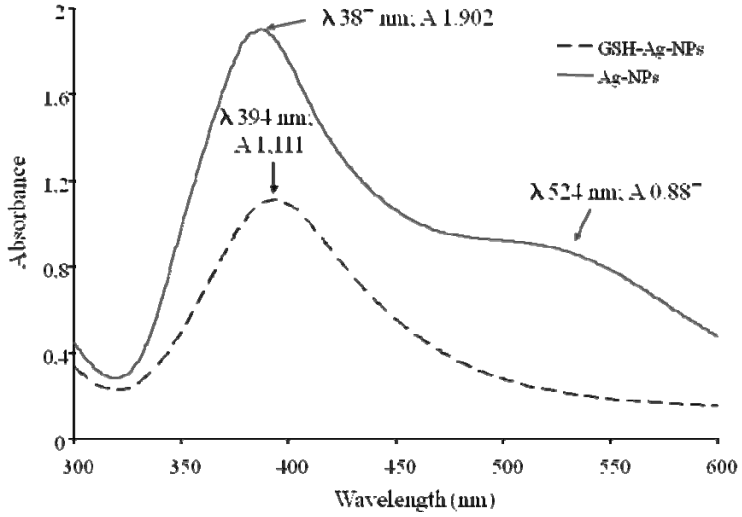

Fig. 4 – UV-Vis spectra of silver nanoparticles before and after the treatment with glutathione (C = 1 mM).

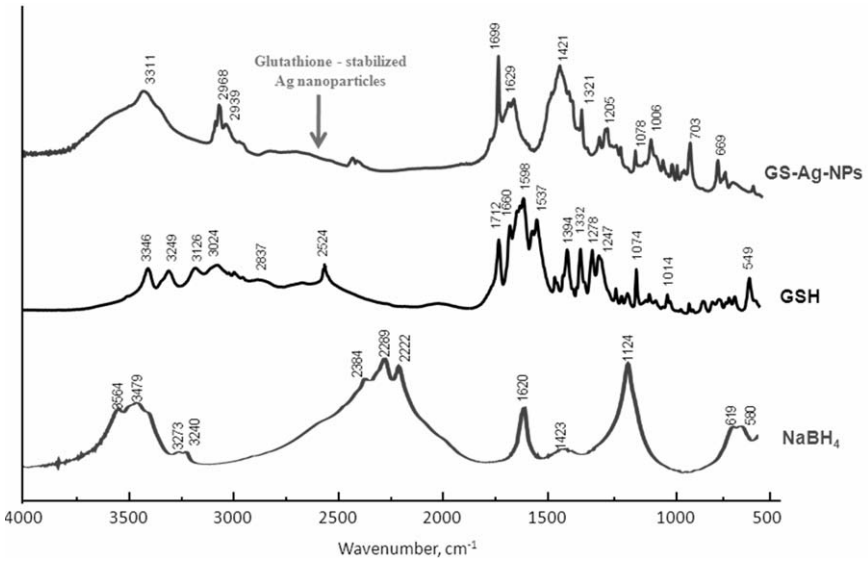

Fig. 5 – FT-IR spectra of glutathione-stabilized silver nanoparticle, free glutathione and sodium borohydride (in KBr solid).

In brief, FT-IR spectrum of GS-Ag-NPs showed several intense and characteristic signals such as those at 1699 cm^{-1}, 1421 cm^{-1}, 2968 cm^{-1}, and 3311 cm^{-1}. Silver nitrate alone had a very intense peak at 1383 cm^{-1}, characteristic to the nitrate ion, and some other important signals at 825 cm^{-1}, 1763 cm^{-1}, 2393 cm^{-1}, and 2731 cm^{-1}, respectively. The most intense signal (1383 cm^{-1}) of $AgNO_3$ did not influence the GS-Ag-NPs spectrum, since it was not found in this spectrum. This suggests that nitrate ion was removed during the GS-Ag-NPs formation. The signal at 1421 cm^{-1} may be generated by the borohydride anion (1423 cm^{-1}), which remained partly bound to the nanoparticle surfaces, and, obviously, by the bound glutathione (1394 cm^{-1}). The peak at around 1629 cm^{-1} may be related to peptide backbone of glutathione, whereas glutathione fingerprint was seen at 1078 cm^{-1} and 1332 cm^{-1}. The vibration of C-H bond has generated two intense peaks at 2918 cm^{-1} and 2939 cm^{-1}, probably due to glutathione adhesion to the nanoparticles.

The most important signal in the GS-Ag-NPs spectrum was found at 1699 cm^{-1} and was assigned to COOH group, which vibrates at 1712 cm^{-1} in the free glutathione molecule.

Atomic Force Microscopy. The size of silver nanoparticles, their morphology and the size distribution were determined by AFM. For this purpose, the Ag-NPs were placed on the special glass plate surface previously examined by AFM, covered by silver nanoparticles suspension, dried and imaged by AFM. Most nanoparticles sized below 20 nm; however they made 50 nm diameter aggregates (Fig. 6).

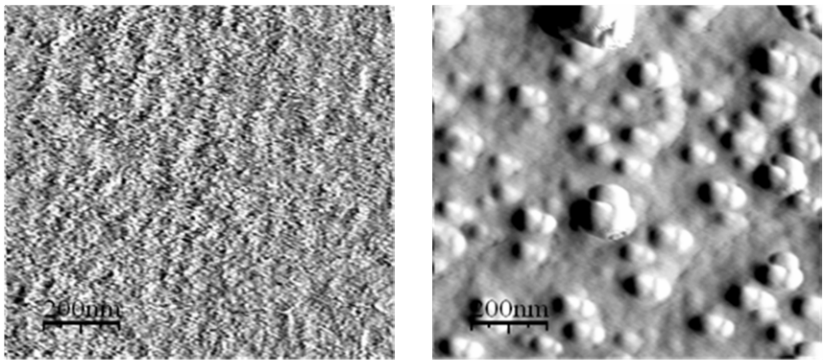

Fig. 6 – AFM images: a) glutathione; b) silver nanoparticles.

Table 1

The effect of Ag-NPs and GS-Ag-NPs on *E. coli* growth expressed as optical density of bacterial suspensions. Optical cell density was measured at 580 nm in triplicate

Treatment/ Concentration	GSH	Ag-Nps	GS-Ag-NPs	D (Tukey test)	Control, H_2O
10^{-6} M	0.678±0.043	0.763±0.054*	0.714±0.047	0.055	0.675±0.021
10^{-5} M	0.648±0.051	0.690±0.052	0.707±0.039	0.049	0.675±0.021
10^{-4} M	0.589±0.041	0.583±0.050*	0.611±0.048	0.065	0.675±0.021

* Statistically significant differences

Morphological analysis of surfaces confirmed the formation of nanoparticles, which crowded when allowed to stay for 48 hours in aqueous suspensions, forming relatively large aggregates (20-150 nm) with different shapes.

Effect of silver nanoparticles on bacterial growth. Biological properties of GS-Ag-NPs were followed at concentrations below 10^{-4} M (Table 1). A volume of 100 ml of the pre-culture has been treated with 5 ml glutathione, and 5 ml colloidal silver nanoparticles stabilized with glutathione. In this respect, three different nanoparticles concentration, 10^{-6} M, 10^{-5} M, and 10^{-4} M were used for treatment. Optical density of pre-culture at 580 nm was only 0.032, whereas that of control was 0.675.

Contrary to the literature data, the free nanoparticles, kept in suspension for 48 hours at concentrations of 10^{-5} M or lower, showed no toxic effect on bacteria studied. Moreover, silver nanoparticles at a concentration of 10^{-6} M had even a stimulatory action on the growth of microorganisms. Generally, Ag-NPs release silver ions, which make an additional contribution to the bactericidal effect.[42, 43] Indeed, Ag-NPs (where silver is present in the Ag^0 form) also contain small concentrations of Ag^+, and both Ag^+ and Ag^0 contribute to the antibacterial activity. The antibacterial effect of Ag-NPs at higher concentrations was found to be similar to that described in the earlier reports.[44] However, only Ag-NPs caused a severe decrease in bacterial density, probably due to aggregation and formation of precipitates on the nanoparticles surface. Therefore, we explained such results by the aggregation effect of silver nanoparticles and not by Ag^+ ions released from them.

The effect of 0.5 mM of colloidal solutions of nanoparticles on *E. coli* sedimentation was followed spectrophotometrically (Table 2). The values corresponding to the optical density of nanoparticles mixed with the suspensions of 21 h-old *E. coli* were subtracted from those of the samples.

Removing the *E. coli* cells was almost complete by centrifugation at 2500-3000 rpm. Since a few cells may be present in the suspensions treated with nanoparticles after the centrifugation at 3000 rpm, over 67% of the Ag-NPs was removed together with *E. coli* cells at this centrifugation rate. Following the same hypothesis, over 53 percent of Ag-NPs was removed by the cells at 2500 rpm. To calculate the percentage of Ag-NPs bound to the removing *E. coli* cells, we took into consideration the difference between the optical density of Ag-NPs treated suspensions and that of the control. Upon adding silver nanoparticles, the optical density of the suspension has decreased by only 6.9%. The centrifugation at 1000 rpm resulted in a decrease in the optical density by 33.1%, which means that the percent of Ag-NPs could be between 0 and 33.1%. On the contrary, GS-Ag-NPs were not significantly released from the suspension by centrifugation at any rate.

Table 2

The effect of 0.5 mM of colloidal solutions of Ag-NPs and GS-Ag-NPs on *E. coli* sedimentation by centrifugation. Optical density of *E. coli* samples mixed with equivalent volumes of 1 mM nanoparticles was measured at 580 nm

Sample	Centrifugation rate (rpm)				
	0	1000	1500	2000	3000
Control	1.32	1.18	0.52	0.10	0.04
Ag-NPs	1.23	0.79	0.18	-0.23	-0.29
GS-Ag-NPs	1.30	1.11	0.49	0.09	0.00

Important biological applications have been or are being developed from silver nanoparticles. However, their cytotoxicity remains a major concern, while different classes of bacteria exhibit different susceptibilities to nanoparticles.[42] Our experiments revealed a behavioral pattern of cytotoxicity as a function of the size, type, and the preparation protocol of nanoparticles. However, the living microorganisms being extremely critical requires the fundamental understanding on the influence of inorganic nanoparticles on cellular growth and functions. During the absorption process, the nanostructures may interact with many biological components.[45] Therefore, the development of predictive models of nanostructure toxicity is needed. We showed here the aggregation process of *E. coli* in the presence of NPs, which depends on the NPs type. Some authors demonstrated that the metal nanoparticles show high tendency for incorporation within bacterial cells with the least possibility of cytotoxicity.[42] The involvement of the nanoparticles on the bacterial physiology might be related to a DNA nanoparticle interaction.

Excessive production of ROS in the cell is known to induce apoptosis.[46, 47] ROS generation has been shown to play an important role in apoptosis induced by treatment with Ag-NPs.[48-50] It is also known that upon association with the nanoparticles, proteins undergo conformational changes, whereas the thickness of the adsorbed protein layer progressively increases with NP size.[48]

MATERIALS AND METHODS

Materials. All chemicals used were of analytical grade or of the highest purity available. All solutions were prepared with milliQ grade water. Silver nitrate and copper sulfate were purchased from Merck, whereas sodium borohydride from Aldrich (Milwaukee, WIS, USA), and glutathione from Fluka (Steinheim, Germany), *Escherichia coli* - DH5α from a T7 Express Sampler, New England, and BioLabs.

Instruments. UV–Vis absorption spectra were acquired on a LIBRA S35 PC UV/VIS spectrophotometer in 1-cm quarz cuvettes. Typically, we measured the optical absorbance in the range from 200 to 700 nm, and recorded the wavelength of the absorbance peak, λ_{max}. Scanning Electron Microscopy was performed using a Quanta 200 microscope equipped with elemental analysis system EDAX. FT-IR spectra were recorded with a Shimadzu Model 8400S FTIR spectrophotometer. Atomic Force Microscopy images were taken with a SPM Solver PRO-M AFM (NT-MTD Co. Zelenograd, Moscow), using the tapping mode.

Methods. *Synthesis of silver nanoparticles was carried out as follows:* A volume of 20 mL of 3 mM sodium borohydride ($NaBH_4$) was poured into an Erlenmeyer flask and cooled in an ice bath on a stir plate. Then, 20 mL of 1 mM silver nitrate was dropped into the stirring $NaBH_4$ solution at approximately 1 drop per second. Separately, a similar suspension of Ag-NPs was prepared, in which 20 mL of 1 mM glutathione was dropwise added. The obtained mixtures were subjected to over constant stirring for two hours.

FT-IR spectroscopy. Both Ag-NPs and the stabilized ones, as well as the precursors were studied using infrared spectroscopy. Spectra were acquired from 1-2 mg sample mixed with KBr and formed into a disk-shaped pellet. All spectra were recorded in the frequency region 500 – 4000 cm^{-1}, under a resolution of 2 cm^{-1}, with a scanning speed of 2 mm sec^{-1}, and 20 scans per sample.

Atomic Force Microscopy. Microscope plates were degreased with alcohol and acetone and dried in an oven at 70 °C for 2 hours. Approximately 50 μl of sample solution was deposited on glass microscope plate, dried at room temperature, in a small covered Petri dish to avoid sample contamination. Samples were then left to dry overnight, and images were taken at room temperature, using "tapping" mode.

Scanning Electron Microscopy. To create an SEM image, the incident electron beam was

scanned in a raster pattern across the sample surface. The emitted electrons were detected for each position in the scanned area by an electron detector. The intensity of the emitted electron signal was displayed as brightness on a cathode ray tube (CRT). By synchronizing the CRT scan to that of the scan of the incident electron beam, the CRT display represents the morphology of the sample surface area scanned by the beam. Magnification of the CRT image is the ratio of the image display size to the sample area scanned by the electron beam.

Testing the biological activity. Test cells of *Escherichia coli* (*E. coli*) were separately grown in 50 mL sterilized Luria Bertani broth medium (LB: 10 g Bacto Tryptone, 5 g Yeast Extract, 5 g NaCl in 1 L; pH adjusted to 7.0) and kept in shaker incubator at 37 °C for 13 hour (overnight incubation). On the subsequent day, the cultures of test organisms were transferred at the rate of 1% in 20 mL LB broth kept in 100 mL Erlenmeyer flasks. Volumes of 2 mL of 1 mM silver nanoparticles as well as the corresponding glutathione stabilized Ag-NPs were carefully placed into each flask, leaving one as a control to track the normal growth of the microbial cells without nanoparticles. Experiments were performed using a colloidal solution of nanoparticles as control (flask containing nanoparticles plus media). The flasks were incubated at 100 rpm and 37 °C in a shaker incubator. The optical density measurements from each flask have been performed every each hour for monitoring the bacterial growth.

In another experiment, pre-cultured *E. coli* was inoculated at 37 °C in the liquid medium (0.33 mL LB 2X, 0.33 mL DH5α and 0.33 mL H_2O) and incubated for 12 hours. The cell density was determined by reading the absorbance at 580 nm with a spectrophotometer.

The effect of silver nanoparticles on *E. coli* has been studied under the same conditions.

Statistics. The data collected were statistically analyzed using Tukey's test.[39]

CONCLUSIONS

The investigation on the formation of silver nanoparticles fits into a more general study of the reactions of biological compounds or microorganisms with metallic ions. Ag-NPs can be utilized for beneficial biological application but significantly they also possess potential to produce ecotoxicity, challenging the ecofriendly nature of nanoparticles. Glutatione functionalization of noble metal Ag-NPs may improve their biological activity.

GSH-Ag NPs described in this work are prepared by reduction of silver nitrate in the presence of GSH. The Ag-NPs thus prepared tend to aggregate together upon addition of Ag^+ due to the strong coordination bond between Ag^+ and $–NH_2$, –COOH of glutathione modifier. The aggregation leads to significant shifting in the absorption spectrum with concomitant visible color changes from yellow to deep orange and provides a simple and inexpensive means for the determination of Ag^+ ions.

The tests made with silver nanoparticles on *E. coli* revealed an aggregation process which could be important to understand their biological properties.

Acknowledgments: This work was supported by the strategic grant POSDRU/159/1.5/S/133652, co-financed by the European Social Fund within the Sectorial Operational Program Human Resources Development 2007–2013.

REFERENCES

1. J. Kreuter and S. Gelperina, *Tumori,* **2008**, *94,* 271-277.
2. J. Su, J. Zhang, L. Liu, Y. Huang and R.P. Mason, *J. Nanosci. Nanotechnol.,* **2008**, *8,* 1174-1177.
3. W.B. Tan, S. Jiang and Y. Zhang, *Biomaterials*, **2007**, *28*, 1565-1571.
4. K.Y. Yoon, J. Hoon Byeon, J. H. Park and J. Hwang, *Sci. Total Environ.*, **2007**, *373*, 572-575.
5. K-T. Yong, M.T. Swihart, H. Ding and P.N. Prasad, *Plasmonics*, **2009**, *4*, 79-93.
6. K. Esumi, T. Hosoya, A. Suzuki and K. Torigoe, *J. Colloid Interface Sci.,* **2000**, *226*, 346-352.
7. S. Link, Z.L. Wang and M.A. El-Sayed, *J. Phys. Chem. B*, **1999**, *103*, 3529- 3533.
8. H. Huang and X. Yang, *Carbohydr. Res.*, **2004**, *339*, 2627- 2631.
9. V. Amendola and M. Meneghetti *J. Mater. Chem.*, **2007**, *17,* 4705-4710.
10. J.P. Abid, A.W. Wark, P.F. Brevet and H.H. Girault, *Chem. Commun.,* **2002**, 792-793.
11. C. He, Y. Yu, X. Hu and A. Larbot, *Appl. Surf. Sci.,* **2002**, *200*, 239-247.
12. L. Yin, Y. Wang, G. Pang, Y. Koltypin and A. Gedanken, *J. Colloid Interface Sci.*, **2002**, *246*, 78-84.
13. M. Brust and C.J. Kiely, *Colloid Surface A,* **2002**, *202*, 175-186.
14. I. Sondi, D.V. Goia and E. Matijevic, *J. Colloid Interface Sci.,* **2003**, *260,* 75-81.
15. T. Hasell, J. Yang, W. Wang, P.D. Brown and S.M. Howdle, *Materials Lett.*, **2007**, *61*, 4906-4910.
16. S.D. Solomon, M.A. Bahadory, A. Jeyarajasingam, S.A. Rutkowsky, C. Boritz and L. Mulfinger, *J. Chem. Edu.*, **2007**, *84*, 322-325.
17. Y.V. Bokshits, G.P. Shevchenko, A.N. Ponyavina and S.K. Rakhmanov, *Colloid J.*, **2004**, *66*, 517-522.
18. D. Van Hyning and C.F. Zukoski, *Langmuir*, **1998**, *14,* 7034-7046.

19. X. Wang, J. Zhuang, Q. Peng and Y.D. Li, *Nature,* **2005**, *437*, 121-124.
20. I. Pastoriza-Santos and L.M. Liz-Marzán, *Langmuir*, **1999**, *15*, 948-951.
21. S. Kéki, J. Török, G. Deák, L. Daróczi and M. Zsuga, *J. Colloid Interface Sci*., **2000**, *229*, 550-553.
22. M. Maillard, P. Huang and L. Brus, *Nano Let.*, **2003**, *3*, 1611-1615.
23. J. Kasthuri, S. Veerapandian and N. Rajendiran, *Colloid Surface B*, **2009**, *68*, 55-60.
24. Y. Sun and Y. Xia, *Science*, **2002**, *298*, 2176-2179.
25. M.S. Cohen, J.M. Stern, A.J. Vanni, R.S. Kelley, E. Baumgart, D. Field, J.A. Libertino and I.C. Summerhayes, *Surg. Infect. (Larchmt.)*, **2007**, *8*, 397-403.
26. D. Cheng, J. Yang and Y. Zhao, *Chin. Med. Equip. J.*, **2004**, *4,* 26-32.
27. H.Y. Lee, H.K. Park, Y.M. Lee, K. Kim and S.B. Park, *Chem. Commun.*, **2007**, *28*, 2959-2961.
28. N. Vigneshwaran, A.A. Kathe, P.V. Varadarajan, R.P. Nachane and R.H. Balasubramanya, *J. Nanosci. Nanotechnol.*, **2007**, *7*, 1893-1897.
29. S.M. Hussain, K.L. Hess, J.M. Gearhart, K.T. Geiss and J.J. Schlager *Toxicol. Vitro,* **2005**, *19,* 975-983.
30. Y-H. Hsin, C-F. Chen, S. Huang, T-S. Shih, P-S. Lai and P.J. Chueh, *Toxicol. Lett.*, **2008**, *179,* 130-139.
31. S. Kim, J.E. Choi, J. Choi, K-H. Chung, K. Park, J. Yi and D-Y Ryu, *Toxicol. Vitro*, **2009**, *23*, 1076-1084.
32. J.L. Elechiguerra, J.L. Burt, J.R. Morones, A. Camacho-Bragado, X. Gao, H.H. Lara and M.J. Yacaman, *J. Nanobiotechnol.*, **2005**, *3*, 6-16.
33. J. Tian, K.K.Y. Wong, C-M. Ho, C-N. Lok, W-Y. Yu, C-M. Che, J-F. Chiu, P.K.H. Tam, *Chem. Med. Chem.*, **2007**, *2*, 129-136.
34. M. Murariu, E.S. Dragan, A. Adochitei, G. Zbancioc and G. Drochioiu, G. *J. Pept. Sci.*, **2011**, *17,* 512-519.
35. J.K. Lim, Y. Kim, S.Y. Lee and S.W. Joo, *Spectrochim. Acta A*, **2008**, *69*, 286-289.
36. B. Marco and B. Thomas, *Langmuir*, **2005**, *21*, 1354-1363.
37. M. Murariu, K. Popa, E.S. Dragan and G. Drochioiu, *Rev. Roum. Chim.*, **2009**, *54*, 741-747.
38. K. Popa, M. Murariu, R. Molnar, G. Schlosser, A. Cecal and G. Drochioiu, *Isot. Environ. Health S.*, **2007**, *43*,105-116.
39. G. V. Snedecor, "Statistical methods applied to experiments in agriculture and biology", The Iowa Stat Univ. Press, U.S.A., 1994, p. 255-274.
40. P.K. Sudeep, S.T.S. Joseph and K.G. Thomas, *J. Am. Chem. Soc.,* **2005**, *127*, 6516-6517.
41. A. Chompoosor, G. Han and V.M. Rotello, *Bioconjugate Chem.,* **2008**, *19*, 1342-1345.
42. Q.L. Feng, J. Wu, G.Q. Chen, F.Z. Cui, T.N. Kim and J.O. Kim, *J. Biomed. Mater. Res.,* **2000**, *52*, 662-668.
43. J.R. Morones, J.L. Elechiguerra, A. Camacho, K. Holt, J.B. Kouri, J.T. Ramirez and M.J. Yacaman, *Nanotechnology,* **2005**, *16*, 2346-2353.
44. S. Shrivastava, T. Bera, A. Roy, G. Singh, P. Ramachandrarao and D. Dash, *Nanotechnology*, **2007**, *18*, 225103-225111.
45. H.C. Fischer and W.C. Chan, *Curr. Opin. Biotechnol.*, **2007**, *18*, 565-571.
46. J.L. Martindale and N.J. Holbrook, *J. Cell Physiol.,* **2002**, *192*, 1-15.
47. J. Sastre, F.V. Pallardó and J. Viña, *IUBMB Life*, **2000**, *49*, 427-435.
48. C. Carlson, S.M. Hussain, A.M. Schrand, L.K. Braydich-Stolle, K.L. Hess, R.L. Jones and J.J. Schlager, *J. Phys. Chem. B*, **2008**, *112*, 13608-13619.
49. P.V. Asharani, G.L.K. Mun, M.P. Hande and S. Valiyaveettil, *ACS Nano*, **2009**, *3*, 279-290.
50. R. Foldbjerg, P. Olesen, M. Hougaard, D.A. Dang, H.J. Hoffmann and H. Autrup, *Toxicol. Lett.*, **2009**, *190*, 156-162.